https://doi.org/10.15407/exp-oncology.2023.01.107

M. Esteves [1,2,*], M. Duarte [2], P.A. Oliveira [3,4], R.M. Gil da Costa [3,5,6,7,8], M.P. Monteiro [9,10], J.A. Duarte [11]

[1] FP-I3ID, FP-BHS, Escola Superior de Saúde Fernando Pessoa, Porto 4200-450, Portugal
[2] Research Center in Physical Activity, Health and Leisure (CIAFEL), Faculty of Sport, University of Porto, 4200-450 Porto, Portugal
[3] Institute for Innovation, Capacity Building and Sustainability of Agri-food Production (Inov4Agro), Centre for Research and Technology of Agro-Environmental and Biological Sciences (CITAB): Clinical Academic Centre,Vila Real, Portugal
[4] Department of Veterinary Sciences, University of Trás-os-Montes and Alto Douro, Vila Real, Portugal
[5] Postgraduate Programme in Adult Health (PPGSAD), Federal University of Maranhão (UFMA), São Luís, Brazil
[6] Molecular Oncology and Viral Pathology Group, Research Center of IPO Porto (CI-IPOP)/RISE@CI-IPOP (Health Research Network), Portuguese Oncology Institute of Porto (IPO Porto), Porto Comprehensive Cancer Center (Porto.CCC), 4200-072 Porto, Portugal
[7] LEPABE — Laboratory for Process Engineering, Environment, Biotechnology and Energy, Faculty of Engineering, University of Porto, Rua Dr. Roberto Frias, 4200-465 Porto, Portugal
[8] Associate Laboratory in Chemical Engineering (ALiCE), Faculty of Engineering, University of Porto, 4200-465 Porto, Portugal
[9] UMIB — Unidade Multidisciplinar de Investigação Biomédica, ICBAS - Instituto de Ciências Biomédicas Abel Salazar, Universidade do Porto, Porto, Portugal
[10] ITR — Laboratory of Integrative and Translocation Research in Population Health, Porto, Portugal
[11] TOXRUN — Toxicology Research Unit, University Institute of Health Sciences, CESPU, CRL, Gandra, Portugal
* Correspondence: Email: ftmarioesteves@gmail.com

SKELETAL MUSCLE SENSITIVITY TO WASTING INDUCED BY UROTHELIAL CARCINOMA

Background. Skeletal muscle wasting is a common phenotypic feature of several types of cancer, and it is associated with functional impairment, respiratory complications, and fatigue. However, equivocal evidence remains regarding the impact of cancer-induced muscle wasting on the different fiber types. **Aim.** The aim of this study was to investigate the impact of urothelial carcinoma induced in mice on the histomorphometric features and collagen deposition in different skeletal muscles. **Materials and Methods.** Thirteen ICR (CD1) male mice were randomly assigned into two groups: exposed to 0.05% N-butyl-N-(4-hydroxybutyl) nitrosamine (BBN) in drinking water for 12 weeks, plus 8 weeks of tap water (BBN, n = 8) or with access to tap water for 20 weeks (CONT, n = 5). Tibialis anterior, soleus,

Citation: Esteves M, Duarte M, Oliveira PA, Gil da Costa RM, Monteiro MP, Alberto Duarte J. Skeletal Muscle Sensitivity to Wasting Induced by Urothelial Carcinoma. *Exp Oncol*. 2023; 44(1): 107-119. https:// doi.org/10.15407/exp-oncology.2023.01.107

and diaphragm muscles were collected from all animals. For cross-sectional area and myonuclear domain analysis, muscle sections were stained with hematoxylin and eosin, and for collagen deposition assessment, muscle sections were stained with picrosirius red. **Results.** All animals from the BBN group developed urothelial preneoplastic and neoplastic lesions, and the tibialis anterior from these animals presented a reduced cross-sectional area ($p < 0.001$), with a decreased proportion of fibers with a higher cross-sectional area, increased collagen deposition ($p = 0.017$), and higher myonuclear domain ($p = 0.031$). BBN mice also showed a higher myonuclear domain in the diaphragm ($p = 0.015$). **Conclusion.** Urothelial carcinoma induced muscle wasting of the tibialis anterior, expressed by a decreased cross-sectional area, higher infiltration of fibrotic tissue, and increased myonuclear domain, which also increased in the diaphragm, suggesting that fast glycolytic muscle fibers are more susceptible to be affected by cancer development.

Keywords: cancer, histology, cross-sectional area, myonuclear domain, collagen deposition.

Cancer is considered one of the most debilitating diseases and its incidence continues to increase, reflecting the growth and aging of the population, as well as the exposure to the main risk factors [1]. In recent years, although the introduction of neoadjuvant chemotherapy and the development of new therapies like antibodies and immune checkpoint inhibitors improved overall survival (OS), cancer remains a common cause of death worldwide [2]. Indeed, about 20% of all cancer-related deaths have been attributed to cachexia, a complex multi-organ syndrome that affects up to 80% of cancer patients [3]. Skeletal muscle loss with structural changes, the most significant events in cancer cachexia, are the main causes of functional impairment and are associated with an increased mortality rate [4]. Indeed, muscle wasting associated with cancer can range from 20 to 70% of muscle loss and is mainly caused by an increase in myofibrillar protein degradation, particularly myosin heavy-chain (MHC), a decrease in protein synthesis, or an imbalance between the two [5]. Consequently, tumor-bearing animals and cancer patients show clinical signs of muscle wasting, with reduced muscle force production and an earlier onset of fatigue [6, 7].

For a long time, chronic inflammation was considered the major mediator of cancer cachexia, involving the up-regulation of pro-inflammatory cytokines, acute phase proteins, and increased insulin resistance, which directly activates the ubiquitin-proteasome system (UPS) and autophagy while inhibiting the synthesis of myofibrillar proteins [8]. However, it seems that the microenvironment of the skeletal muscle may influence its susceptibility to wasting [9]. Indeed, an increased production of reactive oxygen species (ROS) and the reduced expression of antioxidant-related genes are functionally linked to the fast glycolytic muscles catabolism associated with cancer [9]. ROS can act as signaling molecules to regulate cellular viability, but excessive production can activate proteasome-dependent protein degradation by inducing the expression of muscle-specific E3 ligases, muscle atrophy F-box protein (Atrogin-1/MAFbx),and muscle ring-finger protein 1 (MuRF1) [10]. Consequently, there is an increased oxidation of proteins, lipids, and DNA promoting oxidative stress and cellular damage [11]. Thus, considering that the antioxidant capacity is lower in type II fibers due to a heterogeneous mitochondria population and a reduced production of nitric oxide (.NO) and inducible NO synthase (iNOS) [12], glycolytic muscle fibers may experience higher oxidative burden than oxidative fibers in response to cancer-associated wasting [9].

However, conflicting evidence remains to whether there is a selective loss of myofibers or when all skeletal muscles are equally affected by cancer-induced wasting [13]. Interestingly, while some studies observed a selective atrophy of fast glycolytic muscles compared to slow oxidative muscles [14, 15], other authors found that type I fibers were more affected by cancer-induced wasting [16] or that cancer significantly

decreased the cross-sectional area (CSA) of all fibers, independently of the MHC isoform expressed [17]. Although such differences may be partially due to variations in tumor phenotype [18], methodological discrepancies regarding the assessment of muscle wasting among studies could also contributed to these contradictory results because some authors only evaluated the mean weight of muscles [14, 15], while the others only measured the CSA of myofibers without a proper analysis of a potential selective atrophy pattern [19]. Additionally, although the morphologic changes in skeletal muscles, which represent the initial pathological change in wasting are often an occult condition [20], many studies tried to evaluate the potential selective impact of cancer on skeletal muscles using severely cachectic models, which may bias an appropriate assessment because with the installation of clinical signs of cachexia, it is likely that its manifestation became exacerbated to a point that all tissues are affected, hindering an accurate analysis [21].

Therefore, the present study aimed to compare, in a mouse model without clinical signs of cachexia, the impact of urothelial carcinoma (UCC) on the histomorphometric features, specifically the CSA and myonuclear domain (MND), and on the fibrotic tissue deposition of three skeletal muscles with different phenotypic characteristics, i.e., tibialis anterior (TA) composed of type IIb (50%), type IId (18%), type IIa (17%), type I (2%), and hybrid (12%) fibers [22]; soleus (SOL), which shows 70% of fibers expressing only type I MHC isoform, 5% to 10% expressing type IIa isoform and the remaining co-expressing type I and IIa MHC isoforms [23], and the diaphragm, formed by type I (60%), type IId (27%), and type IIa (13%) fibers [22]. We hypothesized that type II fibers and, consequently, TA would be more susceptible to UCC-associated wasting than SOL or diaphragm, thus showing a reduced CSA, higher collagen deposition, and increased MND.

Materials and Methods

Animals and procedures. Thirteen ICR (CD1) male mice were obtained at the age of 4 weeks from Harlan (Barcelona, Spain) and were individually housed in cages with identical floor areas (800 cm^2; Tecniplast, Italy) under controlled conditions of 23 ± 2 °C, 50 ± 10% humidity, and on 12:12-h light-dark cycle. After a week's quarantine, mice were randomly assigned into two groups: exposed to 0.05% N-butyl-N-(4-hydroxybutyl) nitrosamine (BBN) in drinking water in light-impermeable bottles due to its photosensitivity, over the course of 12 weeks plus 8 weeks of tap water without any chemical supplementation (BBN, n = 8) or with access to tap water, without any chemical supplementation over the course of 20 weeks (CONT, n = 5). Due to the increased risk of mortality for BBN mice, n in this group was superior to n in the CONT group in order to face some hypothetical dropouts guarantying a sufficient sample in the BBN group for a proper data analysis. According to the previous studies with this model, tumor burden is expected after 12 weeks of oral exposition to BBN [24, 25]. The animals were kept on a standard diet during the experiment, and body weight (BW) was evaluated weekly. All animal procedures were done according to the protocol approved by the Portuguese Ethics Committee for Animal Experimentation, Direção Geral de Alimentação e Veterinária (licence number 020157; 2014-09-24) in accordance with the European and National Legislation (European Directive 2010/63/EU and National Decree-law 113/2013).

Necropsy. All mice were euthanized 20 weeks after the initial exposure to BBN. The sacrifice was performed by exsanguination through cardiac puncture, under deep anesthesia. TA, SOL, and diaphragm muscles were collected and processed for histology. Their urinary bladders were inflated *in situ* and collected as previously described [26].

Histological analysis. TA, SOL, and diaphragm muscles were fixed (4% (v/v) buffered paraformaldehyde) by diffusion during 24 h and subsequently dehydrated with graded ethanol, cleared in xylene, and embedded in paraffin blocks. The 5 μm-thick sections were cut from paraffin blocks on a Leica 2125 rotary microtome (Leica Microsystems, Germany) and used for histomorphometric analysis and collagen deposition assessment. After fixation for 12 h, the bladders were longitudinally sectioned and further embedded in paraffin. Bladder sections with a thickness of 2 μm were stained with hematoxylin and eosin (H&E), and the mucosal surface was carefully examined for the existence of papillary or nodular lesions. At least one section per animal was evaluated under a light microscope by a pathologist (R.G.C.) to determine the existence of UCC and other urothelial lesions [27]. All the slides were examined in a blind fashion, without prior knowledge of the treatment given to the animals. The lesions found were classified and staged according to the World Health Organization / International Society of Urological Pathology consensus classification of urothelial (transitional cell) neoplasms of the urinary bladder [28]. For CSA and MND analysis, muscle sections were stained with H&E, and for collagen deposition assessment — with Picrosirius Red (SR) according to the method by Sweet and colleagues (for references see [29]). Briefly, the slides were incubated with 0.1% SR in picric acid for 90 min, rinsed in 0.5% acetic acid, dehydrated in ethanol, and cleared in xylene. This technique stains collagen tissue bright red and muscle tissue — yellow.

Samples were analyzed with a light microscope (Axio Imager A1, Carl Zeiss, Germany), with a 40x magnification objective and images recorded with a coupled digital camera (Leica DM4000D, Germany). Images were then examined with ImageJ software (NIH, Bethesda, USA) to measure the CSA of myofibers, collagen deposition, and MND. The myofiber CSA was defined by its individual cross-section area (μm^2), the collagen deposition was evaluated by calculating the percentage of red and yellow areas, and MND was determined by dividing the myofiber CSA by the number of its myonuclei. For consistency, multiple single-frame images (10—15 per section) were acquired from the same muscle section (9 different sections per muscle). In BBN mice, the number of fibers analyzed was 4326 (1497 from TA, 1347 from SOL, and 1482 from diaphragm), while in CONT mice, we assessed 2378 fibers (904 from TA, 816 from SOL, and 658 from diaphragm).

Statistical analysis. Normality and homogeneity of variances were verified by Shapiro — Wilk's and Levene's tests. For normal distributed variables, outcomes were presented as means and standard deviations, and the statistical inference was done through the parametric independent T-test. Without a normal distribution, the outcomes were expressed by median and interquartile range (25—75%), and the statistical analysis was done through the non-parametric Mann — Whitney test. All procedures were performed with SPSS, version 24 (Chicago, IL, USA), and p value below 0.05 was considered statistically significant.

Results and Discussion

All animals from BBN group developed urothelial preneoplastic and neoplastic lesions. No signs of cachexia were evident throughout the entire experimental protocol, as corroborated by the absence of a weight loss ≤5% [30] after 12 weeks of BBN exposure in drinking water followed by 8 weeks of water consumption (Table 1).

TA from BBN mice presented a lower mean fiber CSA compared to CONT (Table 2), which resulted from a decrease in the proportion of fibers with higher CSA (> 1500 μm^2) (Fig. 1). Inversely, there were no significant differences regarding the mean fiber CSA of SOL (Fig. 2) and diaphragm (Fig. 3) muscles between the groups (Table 2). The percentage of collagen deposition

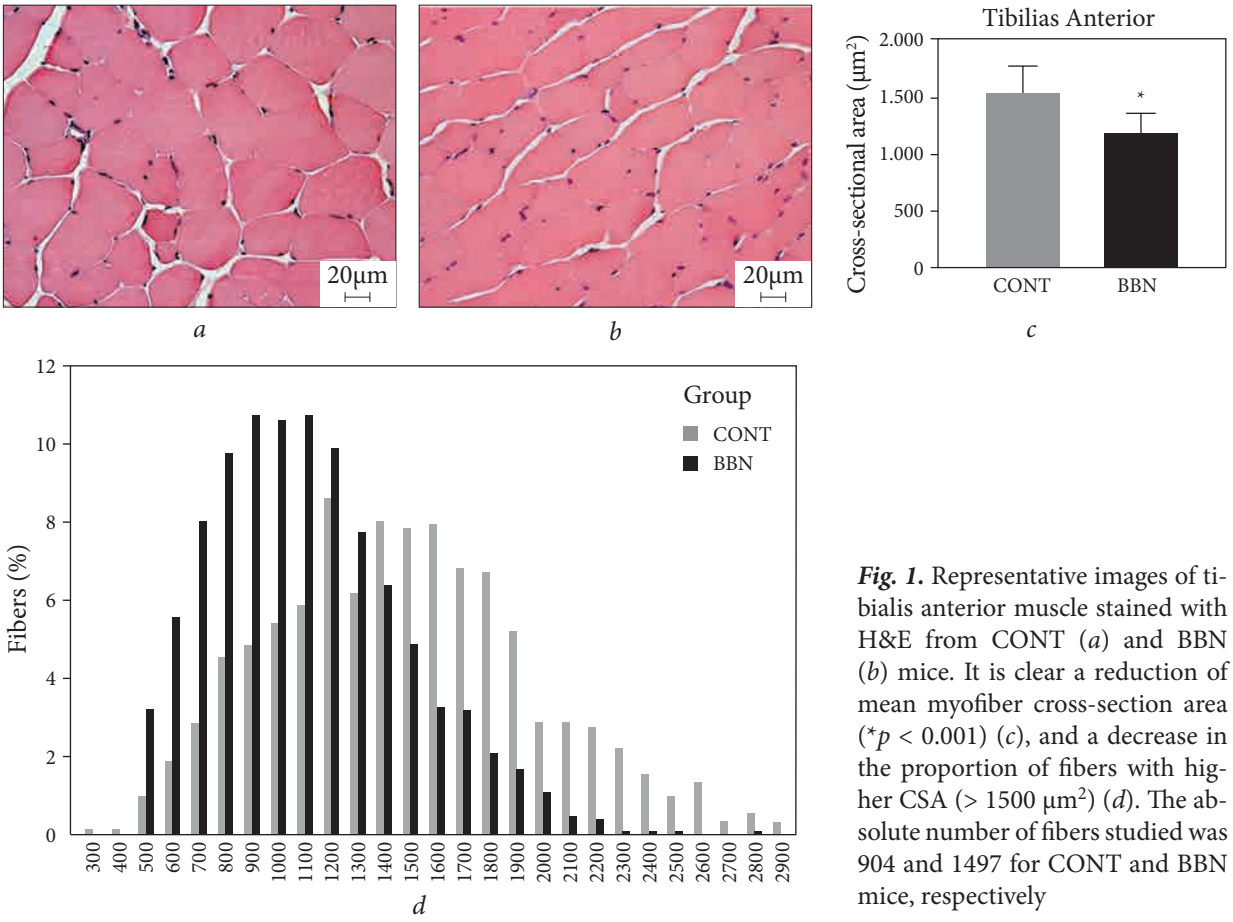

Fig. 1. Representative images of tibialis anterior muscle stained with H&E from CONT (*a*) and BBN (*b*) mice. It is clear a reduction of mean myofiber cross-section area (*$p < 0.001$) (*c*), and a decrease in the proportion of fibers with higher CSA (> 1500 μm²) (*d*). The absolute number of fibers studied was 904 and 1497 for CONT and BBN mice, respectively

was significantly higher in TA muscle from BBN mice compared to CONT (Table 3 and Fig. 4). The percentage of collagen deposition in SOL (Fig. 5) and diaphragm (Fig. 6) muscles did not statistically differ between the groups (Table 3). TA and diaphragm from BBN mice showed a higher MND compared to CONT. In contrast, SOL muscle did not present any difference in the MND between the groups studied (Table 4).

The results of the present study showed that a mouse model of UCC significantly induced wasting of TA with a decreased myofiber CSA, increased collagen deposition, and higher MND. Moreover, we found that, although there were no changes in the diaphragmatic myofiber CSA and fibrotic tissue infiltration, UCC promoted an important increase in MND of this muscle. Contrarily, SOL muscle did not show any signs of wasting associated with UCC. Interestingly, by distributing the myofibers according to CSA categories, we observed in TA that fibers with higher CSA were more affected by UCC, indicating its particular susceptibility to wasting. This observation is in agreement with the previous studies reporting that fast-glycolytic muscles seem to be more prone to cancer-induced wasting than slow-oxidative muscles [14, 15]. In-

Table 1. **Body weight (mean ± standard deviation)**

Body weight	Body weight (g)	
	CONT	BBN
Baseline	24.14 ± 2.04	25.80 ± 0.85
Final	28.07 ± 3.83	27.69 ± 0.98

deed, the study of Jullienne et al. [14] focusing on different hindlimb muscles found that SOL was the only skeletal muscle unaffected by peritoneal carcinosis. The remaining muscles, including extensor digitorum longus (EDL), gastrocnemius (GAST), and TA had a significant weight reduction, ranging from 7 to 10% loss. Similarly, in a C-26 tumor model, Acharyya et al. [15] observed a significant wasting of TA, with minimal change in SOL muscle weight. However, although the assessment of muscle weight might be considered an operative variable to evaluate the occurrence of muscle atrophy, as this method does not differentiate the muscle fibers/connective tissue contributions, it is not adequate for the evaluation of a potential myofiber-selective targeting [31]. Therefore, as the skeletal muscle is not exclusively composed of only one type of fibers, without identifying myofibers and measuring their CSA with a histogram to assess the

Table 2. **Cross-section area**

Muscle	Cross-section area (μm²)				
	CONT		BBN		*p*
	Mean ± SD	95% CI	Mean ± SD	95% CI	
Tibialis anterior	1518.23 ± 122.82	1365.74; 1670.73	1166.93 ± 99.99	1083.34; 1250.53	0.0001
Diaphragm	696.24 ± 54.39	628.71; 763.78	676.88 ± 28.77	652.83; 700.94	0.414
Soleus	664.20 ± 42.94	610.88; 717.52	640.02 ± 43.31	603.81; 676.22	0.347

Note: CI — confidence interval; SD — standard deviation.

Table 3. **Collagen deposition**

Muscle	Cross-section area (μm²)				
	CONT		BBN		*p*
	Mean ± SD	95% CI	Mean ± SD	95% CI	
Tibialis anterior	4.47 ± 0.41	3.96; 4.99	5.08 ± 0.36	4.78; 5.37	0.017
Diaphragm	3.89 ± 0.54	3.21; 4.57	4.32 ± 0.44	3.95; 4.70	0.143
Soleus	3.76 ± 0.57	3.05; 4.47	3.98 ± 0.54	3.53; 4.43	0.508

Note: CI — confidence interval; SD — standard deviation.

Table 4. **Myonuclear domain**

Muscle	Myonuclear domain (μm²)				
	CONT		BBN		*p*
	Mean ± SD	95% CI	Mean ± SD	95% CI	
Tibialis anterior	569.79 ± 116.36	425.31; 714.26	729.45 ± 111.67	636.09; 822.81	0.031
Diaphragm	316.77 ± 82.28	214.60; 441.93	445.05 ± 75.86	381.63; 508.46	0.015
Soleus	334.35 ± 103.80	205.46; 463.24	419.67 ± 65.22	365.15; 474.19	0.093

Note: CI — confidence interval; SD — standard deviation.

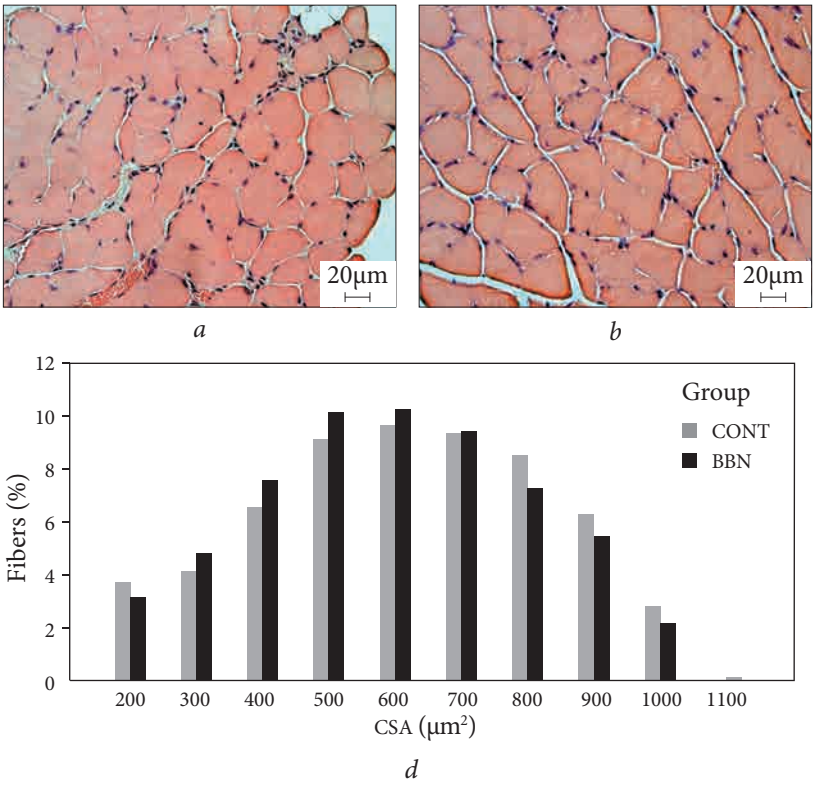

Fig. 2. Representative images of soleus muscle stained with H&E from CONT (*a*) and BBN (*b*) mice. There were no differences regarding mean fiber CSA between the groups (*c* and *d*). The absolute number of fibers studied was 816 and 1347 for CONT and BBN mice, respectively

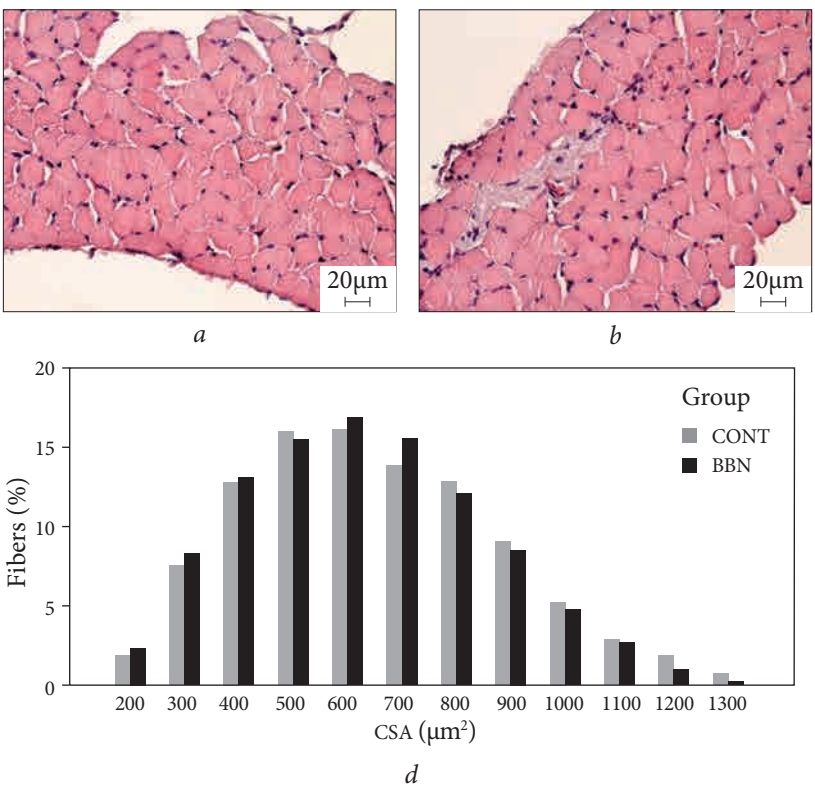

Fig. 3. Representative images of diaphragm muscle stained with H&E from CONT (*a*) and BBN (*b*) mice. There were no differences regarding mean fiber CSA between the groups (*c* and *d*). The absolute number of fibers studied was 658 and 1482 for CONT and BBN mice, respectively

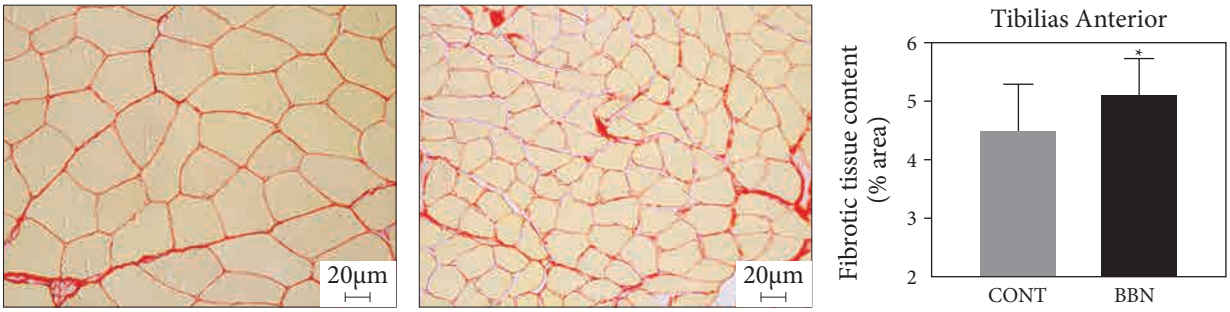

Fig. 4 Representative images of tibialis anterior muscle stained with picrosirius red from CONT (*a*) and BBN (*b*) mice. The mean percentage of collagen deposition is higher in BBN mice (*$p = 0.017$) (*c*)

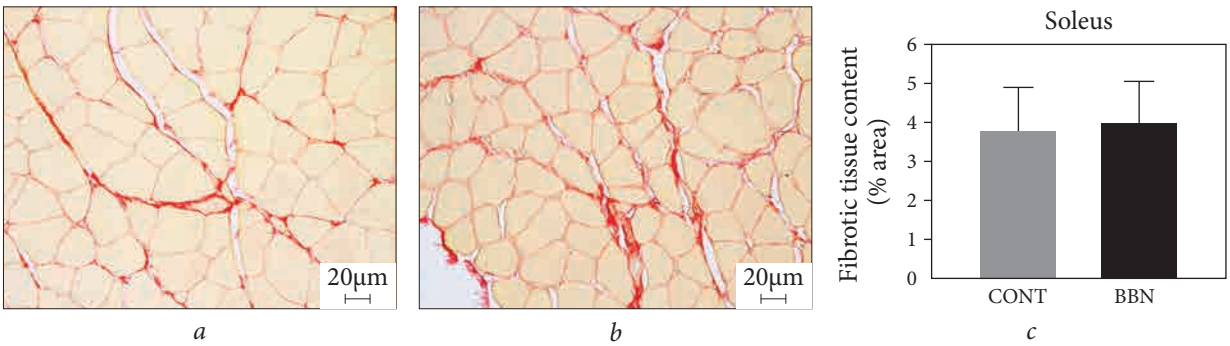

Fig. 5. Representative images of soleus muscle stained with picrosirius red from CONT (*a*) and BBN (*b*) mice. The percentage of collagen deposition was not different between groups (*c*)

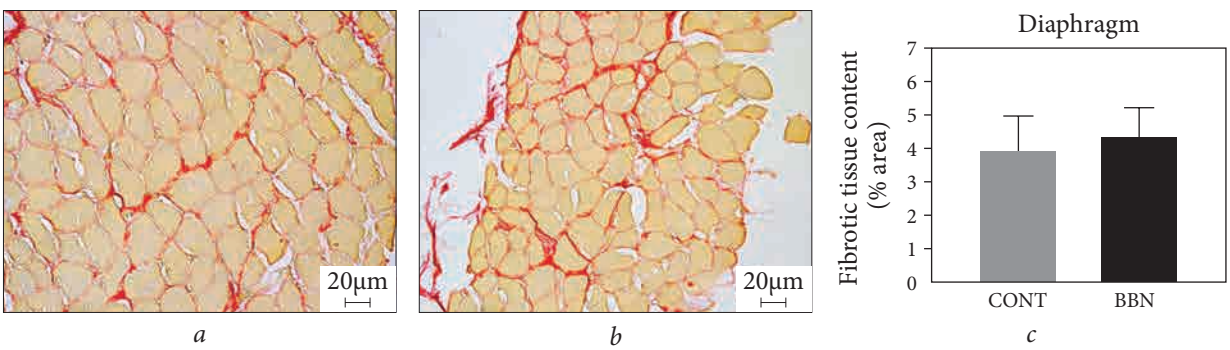

Fig. 6. Representative images of diaphragm muscle stained with picrosirius red from CONT (*a*) and BBN (*b*) mice. The percentage of collagen deposition was not different between groups (*c*)

most atrophied ones, it remains inconclusive if the weight reduction of the skeletal muscles observed in that studies is in fact attributed to a specific wasting of the type II fibers.

Aulino et al. [17] also evaluated the impact of a C-26 tumor model on the histomorphometric properties of EDL, TA, and SOL from BALB/c mice and, contrary to our results, found that all muscles showed signs of wasting. Nonetheless, since the tumor-bearing mice assessed were severely cachectic, with a 30% reduction in their BW, this means that the animals presented

an advanced pro-catabolic state, which was not suitable for this type of comparison. Corroborating this notion, other two studies involving severely cachectic C-26 mice showed a similar reduction in the muscle weight for fast-glycolytic (EDL and GAST) and slow-oxidative (SOL) muscles, highlighting the development of a systemic wasting pattern in this later stage of the disease [16, 32].

Moreover, two studies recognized the occurrence of diaphragmatic dysfunction in cachectic C-26 mice [33, 34]. Indeed, Roberts et al. [33] showed that the mean CSA of all diaphragm fibers decreased by 26%, while Murphy et al. [34] reported a 10% lower maximum specific force and lower absolute force production of diaphragm from severely cachectic mice. The diaphragm is a chronically active muscle and, although being composed mainly of type I fibers, it also expresses IIa and IId fibers, where the high amount of oxidative fibers provide sustained respiration at rest and type IId fibers allow increasing respiratory rate observed during physical exercise or during high-power output that occurs in sneezing and coughing [35]. Thus, according to our results, it seems that before the initiation of clinical signs of muscle wasting, the continuous activity of diaphragm for ventilation as well as of SOL for postural control during standing and walking may provide an additional protection from the catabolic systemic environment. However, as the progression to a more severe cachectic phenotype is characterized by an intense systemic catabolism, increased energy expenditure, insulin resistance, anemia, and hypogonadism [30], these disturbing factors favor the installation of a general wasting pattern, hindering a rigorous evaluation of the susceptibility across different muscles and/or different fibers [36].

Additionally, in our study, the development of UCC also induced an increased collagen deposition in TA, but not in diaphragm or SOL. Indeed, skeletal muscle fibrosis is a common hallmark of chronic muscle wasting disorders. Considering that an excessive accumulation of extracellular matrix (ECM) components, particularly collagen, in skeletal muscle results in reduced contractility, besides a decreased CSA [37], the clinical guidelines highlighted the increased fibrotic tissue area as an important cofactor to define a pathological condition [38]. Interestingly, in a recent study, Judge et al. [39] revealed that the rectus abdominis from cachectic patients with pancreatic ductal adenocarcinoma had higher levels of collagen deposition compared to non-cancer control subjects that correlated with lymph node metastasis and decreased OS. Therefore, as tissue fibrosis is the end result of a cascade of events occurring from tissue injury to necrosis via inflammation resulting in the permanent scar formation [40], the replacement of muscle fibers with connective tissue represents a relevant outcome that must be assessed to predict cancer progression [39]. Furthermore, such replacement is a known consequence of impaired muscle regeneration following muscle injury [40]. Indeed, the heterogeneity of satellite cells (SCs) can promote important differences in the regenerative capacity of slow oxidative and fast glycolytic skeletal muscles. Since a higher quantity of SCs is associated with the capillary density [41] and myonuclear number [42], it can be assumed that type I fibers have a five to six greater concentration of SCs compared to type II fibers [43]. Indeed, the MND has been found to be different according to the oxidative capacity of the fibers and the MHC expressed, with type I fibers having smaller MND than type II fibers [44]. Curiously, several studies demonstrated that reduction of the myonuclear number during muscle atrophy was not always proportional to the decrease in the myofiber CSA, resulting in significant changes in the MND size [45—47]. The results of the present study corroborate this idea by showing an increased MND in TA and diaphragm from BBN mice but not in SOL. Therefore, considering that each myonucleus controls

the transcription and, consequently, the protein synthesis of a limited amount of cytoplasm, an increased MND means that the same myonucleus is responsible for a higher cytoplasmic volume, suggesting that the regenerative potential of TA and diaphragm muscles may have been compromised [49].

The present study provides fundamental knowledge regarding how UCC selectively impacts different skeletal muscles and their fibers, which should be taken in account in the clinical setting when addressing the prevention and management of cancer-associated muscle wasting and cachexia. In the future, studies addressing potential interventions that may prevent or overcome these findings and evaluating the long-term effects of UCC on the respiratory muscles are welcome. However, as muscle samples were fixed and further embedded in paraffin blocks, it was not possible to process fresh cuts for identification of different muscle fiber types. Nonetheless, considering that the fiber type composition of each muscle is well described in the literature [22, 23], the differences found between the muscles in the present study point to a higher susceptibility of fast glycolytic TA muscle, particularly the fibers with higher CSA, to the UCC-induced muscle atrophy.

In conclusion, the results indicate that under the condition of UCC, local skeletal muscle's features exert influence on the installation of wasting. The fast glycolytic TA muscle, particularly the fibers with higher CSA, seems to be more prone to the atrophic signal, compared to the smaller CSA fibers and to chronically active muscles like SOL and diaphragm, reinforcing the notion of a heterogeneous response to cancer-induced muscle wasting. Although TA presented an increased MND and a higher deposition of fibrotic tissue, indicating a more demanding muscle's regeneration process, the MND of diaphragm was also superior, suggesting that its regenerative capacity may be compromised, thus raising some concerns about the long-term respiratory impact of UCC.

Acknowledgements

The authors would like to thank Mrs. Celeste Resende for her technical support. This research was funded by the FCT-Portuguese Foundation for Science and Technology, under Project UIDB/04033/2020 and by Base Funding — UIDB/00511/2020 of the Laboratory for Process Engineering, Environment, Biotechnology and Energy (LEPABE) funded by national funds through the FCT/MCTES (PIDDAC).

REFERENCES

1. Bray F, Ferlay J, Soerjomataram I, et al. Global cancer statistics 2018: GLOBOCAN estimates of incidence and mortality worldwide for 36 cancers in 185 countries. CA Cancer J Clin 2018; **68**: 394-424. doi: 10.3322/caac.21492
2. Arnold M, Rutherford MJ, Bardot A, et al. Progress in cancer survival, mortality, and incidence in seven high-income countries 1995-2014 (ICBP SURVMARK-2): a population-based study. Lancet Oncol 2019; **20**: 1493-1505. doi: 10.1016/S1470-2045(19)30456-5
3. Fearon KC. Cancer cachexia: developing multimodal therapy for a multidimensional problem. Eur J Cancer 2008; **44**: 1124-1132. doi: 10.1016/j.ejca.2008.02.033
4. Argiles JM, Busquets S, Stemmler B, et al. Cancer cachexia: understanding the molecular basis. Nat Rev Cancer 2014; **14**: 754-762. doi: 10.1038/nrc3829
5. Eley HL, Tisdale MJ. Skeletal muscle atrophy, a link between depression of protein synthesis and increase in degradation. J Biol Chem 2007; **282**: 7087-7097. doi: 10.1074/jbc.M610378200
6. Toledo M, Busquets S, Sirisi S, et al. Cancer cachexia: physical activity and muscle force in tumour-bearing rats. Oncol Rep 2011; **25**: 189-193
7. Bower JE. Cancer-related fatigue—mechanisms, risk factors, and treatments. Nat Rev Clin Oncol 2014; **11**: 597-609. doi:10.1038/nrclinonc.2014.127

8. Biolo G, Cederholm T, Muscaritoli M. Muscle contractile and metabolic dysfunction is a common feature of sarcopenia of aging and chronic diseases: from sarcopenic obesity to cachexia. Clin Nutr 2014; **33**: 737-748. doi:10.1016/j.clnu.2014.03.007
9. Hardee JP, Montalvo RN, Carson JA. Linking cancer cachexia-induced anabolic resistance to skeletal muscle oxidative metabolism. Oxid Med Cell Longev 2017; **2017**: 8018197. doi: 10.1155/2017/8018197
10. Li YP, Chen Y, Li AS, et al. Hydrogen peroxide stimulates ubiquitin-conjugating activity and expression of genes for specific E2 and E3 proteins in skeletal muscle myotubes. Am J Physiol Cell Physiol 2003; **285**: C806-C812. doi: 10.1152/ajpcell.00129.2003
11. Ott M, Gogvadze V, Orrenius S, et al. Mitochondria, oxidative stress and cell death. Apoptosis 2007; **12**: 913-922. doi: 10.1007/s10495-007-0756-2
12. Yu Z, Li P, Zhang M, et al. Fiber type-specific nitric oxide protects oxidative myofibers against cachectic stimuli. PLoS One 2008; **3**: e2086. doi:10.1371/journal.pone.0002086
13. Johns N, Hatakeyama S, Stephens NA, et al. Clinical classification of cancer cachexia: phenotypic correlates in human skeletal muscle. PLoS One 2014; **9**: e83618. doi: 10.1371/journal.pone.0083618
14. Julienne CM, Dumas JF, Goupille C, et al. Cancer cachexia is associated with a decrease in skeletal muscle mitochondrial oxidative capacities without alteration of ATP production efficiency. J Cachexia Sarcopenia Muscle 2012; **3**: 265-275. doi: 10.1007/s13539-012-0071-9
15. Acharyya S, Ladner KJ, Nelsen LL, et al. Cancer cachexia is regulated by selective targeting of skeletal muscle gene products. J Clin Invest 2004; **114**: 370-378. doi: 10.1172/JCI20174
16. Hiroux C, Dalle S, Koppo K, et al. Voluntary exercise does not improve muscular properties or functional capacity during C26-induced cancer cachexia in mice. J Muscle Res Cell Motil 2021; **42**: 169-181. doi: 10.1007/s10974-021-09599-6
17. Aulino P, Berardi E, Cardillo VM, et al. Molecular, cellular and physiological characterization of the cancer cachexia-inducing C26 colon carcinoma in mouse. BMC Cancer 2010; **10**: 363. doi: 10.1186/1471-2407-10-363
18. Monitto CL, Berkowitz D, Lee KM, et al. Differential gene expression in a murine model of cancer cachexia. Am J Physiol Endocrinol Metab 2001; **281**: E289-E297. doi:10.1152/ajpendo.2001.281.2.E289
19. Marin-Corral J, Fontes CC, Pascual-Guardia S, et al. Redox balance and carbonylated proteins in limb and heart muscles of cachectic rats. Antioxid Redox Signal 2010; **12**: 365-380. doi: 10.1089/ars.2009.2818
20. Fearon KC, Glass DJ, Guttridge DC. Cancer cachexia: mediators, signaling, and metabolic pathways. Cell Metab 2012; **16**: 153-166. doi: 10.1016/j.cmet.2012.06.011
21. Li P, Waters RE, Redfern SI, et al. Oxidative phenotype protects myofibers from pathological insults induced by chronic heart failure in mice. Am J Pathol 2007; **170**: 599-608. doi: 10.2353/ajpath.2007.060505
22. Talmadge RJ, Roy RR. Electrophoretic separation of rat skeletal muscle myosin heavy-chain isoforms. J Appl Physiol (1985) 1993; **75**: 2337-2340
23. Caiozzo VJ, Baker MJ, Baldwin KM. Novel transitions in MHC isoforms: separate and combined effects of thyroid hormone and mechanical unloading. J Appl Physiol (1985) 1998; **85**: 2237-2248. doi: 10.1152/jappl.1998.85.6.2237
24. Vasconcelos-Nobrega C, Pinto-Leite R, Arantes-Rodrigues R, et al. In vivo and in vitro effects of RAD001 on bladder cancer. Urol Oncol 2013; **31**: 1212-1221. doi: 10.1016/j.urolonc.2011.11.002
25. Ferreira R, Neuparth MJ, Nogueira-Ferreira R, et al. Exercise training impacts cardiac mitochondrial proteome remodeling in murine urothelial carcinoma. Int J Mol Sci 2018; **20**: 127 doi: 10.3390/ijms20010127
26. Oliveira PA, Vasconcelos-Nobrega C, Gil da Costa RM, et al. The N-butyl-N-4-hydroxybutyl nitrosamine mouse urinary bladder cancer model. Methods Mol Biol 2018; **1655**: 155-167. doi: 10.1007/978-1-4939-7234-0_13
27. Oliveira PA, Gil da Costa RM, Vasconcelos-Nobrega C, et al. Challenges with in vitro and in vivo experimental models of urinary bladder cancer for novel drug discovery. Expert Opin Drug Discov 2016; **11**: 599-607. doi: 10.1080/17460441.2016.1174690
28. Epstein JI, Amin MB, Reuter VR, et al. The World Health Organization/International Society of Urological Pathology consensus classification of urothelial (transitional cell) neoplasms of the urinary bladder. Bladder Consensus Conference Committee. Am J Surg Pathol 1998; **22**: 1435-1448. doi: 10.1097/00000478-199812000-00001
29. Bovolini A, Garcia J, Andrade MA, et al. Relative contribution of fat diet and physical inactivity to the development of metabolic syndrome and non-alcoholic fat liver disease in Wistar rats. Physiol Behav 2020; **225**: 113040. doi: 10.1016/j.physbeh.2020.113040

30. Fearon K, Strasser F, Anker SD, et al. Definition and classification of cancer cachexia: an international consensus. Lancet Oncol 2011; **12**: 489-495. doi: 10.1016/S1470-2045(10)70218-7
31. McGregor RA, Cameron-Smith D, Poppitt SD. It is not just muscle mass: a review of muscle quality, composition and metabolism during ageing as determinants of muscle function and mobility in later life. Longev Healthspan 2014; **3**: 9. doi: 10.1186/2046-2395-3-9
32. Roberts BM, Frye GS, Ahn B, et al. Cancer cachexia decreases specific force and accelerates fatigue in limb muscle. Biochem Biophys Res Commun 2013; **435**: 488-492. doi: 10.1016/j.bbrc.2013.05.018
33. Roberts BM, Ahn B, Smuder AJ, et al. Diaphragm and ventilatory dysfunction during cancer cachexia. FASEB J 2013; **27**: 2600-2610. doi: 10.1096/fj.12-222844
34. Murphy KT, Chee A, Trieu J, et al. Importance of functional and metabolic impairments in the characterization of the C-26 murine model of cancer cachexia. Dis Model Mech 2012; **5**: 533-545. doi: 10.1242/dmm.008839
35. Gransee HM, Mantilla CB, Sieck GC. Respiratory muscle plasticity. Compr Physiol 2012; **2**: 1441-1462. doi: 10.1002/cphy.c110050
36. Aversa Z, Costelli P, Muscaritoli M. Cancer-induced muscle wasting: latest findings in prevention and treatment. Ther Adv Med Oncol 2017; **9**: 369-382. doi: 10.1177/1758834017698643
37. Delaney K, Kasprzycka P, Ciemerych MA, et al. The role of TGF-beta1 during skeletal muscle regeneration. Cell Biol Int 2017; **41**: 706-715. doi: 10.1002/cbin.10725
38. Lieber RL, Ward SR. Cellular mechanisms of tissue fibrosis. 4. Structural and functional consequences of skeletal muscle fibrosis. Am J Physiol Cell Physiol 2013; **305**: C241-C252. doi: 10.1152/ajpcell.00173.2013
39. Judge SM, Nosacka RL, Delitto D, et al. Skeletal muscle fibrosis in pancreatic cancer patients with respect to survival. JNCI Cancer Spectr 2018; **2**: pky043. doi: 10.1093/jncics/pky043
40. Mann CJ, Perdiguero E, Kharraz Y, et al. Aberrant repair and fibrosis development in skeletal muscle. Skelet Muscle 2011; **1**: 21. doi: 10.1186/2044-5040-1-21
41. Christov C, Chretien F, Abou-Khalil R, et al. Muscle satellite cells and endothelial cells: close neighbors and privileged partners. Mol Biol Cell 2007; **18**: 1397-1409. doi: 10.1091/mbc.e06-08-0693
42. Pallafacchina G, Blaauw B, Schiaffino S. Role of satellite cells in muscle growth and maintenance of muscle mass. Nutr Metab Cardiovasc Dis 2013; **23** Suppl 1: S12-S18. doi: 10.1016/j.numecd.2012.02.002
43. Gibson MC, Schultz E. The distribution of satellite cells and their relationship to specific fiber types in soleus and extensor digitorum longus muscles. Anat Rec 1982; **202**: 329-337. doi: 10.1002/ar.1092020305
44. Liu JX, Hoglund AS, Karlsson P, et al. Myonuclear domain size and myosin isoform expression in muscle fibres from mammals representing a 100,000-fold difference in body size. Exp Physiol 2009; **94**: 117-129. doi: 10.1113/expphysiol.2008.043877
45. Dupont-Versteegden EE, Murphy RJ, Houle JD, et al. Activated satellite cells fail to restore myonuclear number in spinal cord transected and exercised rats. Am J Physiol 1999; **277**: C589-C597. doi: 10.1152/ajpcell.1999.277.3.C589
46. Zhong H, Roy RR, Siengthai B, et al. Effects of inactivity on fiber size and myonuclear number in rat soleus muscle. J Appl Physiol (1985) 2005; **99**: 1494-1499. doi: 10.1152/japplphysiol.00394.2005
47. Bruusgaard JC, Gundersen K. In vivo time-lapse microscopy reveals no loss of murine myonuclei during weeks of muscle atrophy. J Clin Invest 2008; **118**: 1450-1457. doi: 10.1172/JCI34022
48. van Wessel T, de Haan A, van der Laarse WJ, et al. The muscle fiber type-fiber size paradox: hypertrophy or oxidative metabolism? Eur J Appl Physiol 2010; **110**: 665-694. doi: 10.1007/s00421-010-1545-0
49. Wang Y, Pessin JE. Mechanisms for fiber-type specificity of skeletal muscle atrophy. Curr Opin Clin Nutr Metab Care 2013; **16**: 243-250. doi: 10.1097/MCO.0b013e328360272d

Submitted: December 10, 2021.

М. Естевес, М. Дуарте, П.А. Олівейра,
Р.М. Жіл да Коста, М.П. Монтейро, Ж.А. Дуарте

Вища медична школа Фернандо Пессоа, Порто, Португалія
Спортивний факультет університету Порто, Португалія
Інститут інновацій, Дослідно-технологічний центр сільськогосподарських
та біологічних досліджень, Віла-Реал, Португалія
Португальський онкологічний інститут, Порто, Португалія
Федеральний університет Мараньян, Сан-Луїс, Бразилія
Сектор мультидисциплінарних біомедичних досліджень,
Інститут біомедичних наук Абеля Салазара, Університет Порто, Порто, Португалія
TOXRUN — сектор токсикологічних досліджень, університетський
інститут медичних наук, CESPU, CRL, Гандра, Португалія

ЧУТЛИВІСТЬ СКЕЛЕТНИХ М'ЯЗІВ ДО ВИСНАЖЕННЯ, ІНДУКОВАНОГО УРОТЕЛІАЛЬНОЮ КАРЦИНОМОЮ

Стан питання. Виснаження скелетних м'язів є загальною фенотиповою рисою кількох різновидів раку та асоціюється з функціональними порушеннями, ускладненням дихання і загальним виснаженням. Нез'ясованим лишається питання щодо особливостей цього процесу для різних типів м'язових волокон. **Мета.** Дослідити вплив індукованої у мишей уротеліальної карциноми на гістоморфометричні параметри та відкладення колагену в різних скелетних м'язах. **Матеріали та методи.** Самцям мишей ICR (CD1) впродовж 12 тижнів додавали до питної води 0,05% N-бутил-N-(4-гідроксибутил) нітрозамін, після чого впродовж 8 тижнів давали питну воду без канцерогену (n = 8). В контролі (n = 5) мишам впродовж 20 тижнів давали питну воду без канцерогену. Досліджували передній великогомілковий, камбалоподібний та діафрагмальний м'язи. Зрізи м'язової тканини забарвлювали гематоксиліном-еозином для визначення площі поперечного перерізу міофібрил і розмірів міонуклеарного домену та пікросиріусом червоним для визначення відкладення колагену. **Результати.** Пренеопластичні та непластичні ураження розвивались у всіх мишей, які отримували канцероген. У них відзначали зменшення поперечного перерізу міофібрил переднього великогомілкового м'яза ($p < 0{,}001$), збільшення відкладення колагену ($p = 0{,}017$) та збільшення розмірів міонуклеарного домену ($p = 0{,}031$). Збільшення розмірів міонуклеарного домену відзначали також у діафрагмальному м'язі ($p = 0{,}015$). **Висновки.** У мишей з уротеліальною карциномою спостерігається виснаження переднього великогомілкового м'яза, що проявляється зменшенням поперечного перерізу міофібрил м'яза, підвищенням інфільтрації фібротичної тканини та збільшенням розмірів міонуклеарного домену. Останнє має місце також у діафрагмальному м'язі. Можна припустити, що більш сприйнятливими до індукованого розвитком пухлини виснаження є м'язові волокна з підвищеним рівнем гліколізу.

Ключові слова: гістологія, уротеліальна карцинома, поперечний переріз м'язових волокон, міонуклеарний домен, відкладення колагену.